

## THREE-DIMENSIONAL THERMO-MECHANICAL MODEL WITH VARIABLE DENSITY IN APPLICATION TO SEMI-SOLID ROLLING OF SLABS

Marcin HOJNY, Dariusz JEĐRZEJCZYK, Mirosław GŁOWACKI

*AGH University of Science and Technology, Cracow, Poland, EU, [mhojny@metal.agh.edu.pl](mailto:mhojny@metal.agh.edu.pl)*

### Abstract

The paper deals with three dimensional computer simulation of rolling process of plates with mushy zone. The model became a basis for a computer simulation system of soft reduction process, which is the final phase of continuous casting technology. The presented model focuses on three basic phenomena: mechanical, thermal and density changes, which describe deformation of both solid and semi-solid regions of steel slabs. As a result of the authors' work, three models have been developed. The first of them is a mathematical model of temperature evolution at the final stage of solidification. The second, mechanical model allows for the description of plastic flow kinetics in solid and semi-solid regions. The third is a mathematical model allowing the prediction of material density changes during the final stage of material solidification with simultaneous plastic deformation. Density is one of the decisive factors affecting both the temperature change model and the mechanical model. Its changes, which occur with the progressive transformation of steel aggregation state, are ruled by three main factors: formation of the solid phase due to solidification of the body, thermal shrinkage of solid and liquid phases and displacement of the liquid phase in the matrix of porous solid phase.

**Keywords:** Semi-Solid State, Finite Elements Method, Mathematical Modelling

### 1. INTRODUCTION

In the recent two decades, researchers have paid much attention to semi-solid forming (SSF). The reason of being under attention is higher production rate and lower energy consumption rather than conventional forming processes. The mathematical and experimental modelling of mushy steel deformation is an innovative topic regarding the very high temperature range deformation processes. Tracing the related papers published in the past 10-15 years, one can find many papers regarding experimental results [1] and modeling [2] for non-ferrous metals tests, but the papers deal mainly with tixotrophy. The first results regarding steel deformation at extra high temperature were presented in the past few years [3,4]. The situation is caused by the very high level of steel liquidus and solidus temperatures in comparison with non-ferrous metals. The deformation tests for non-ferrous metals are much easier. Thixoforming or semi-solid metal forming offers many advantages in comparison with casting and conventional forging. However, because of the highmelting temperature and other related difficulties, there is relatively less amount of experimental data and investigations available on steels. Direct slab casting technology has been introduced in 1985 by Schloeman Siemag AG (SMS) and has successfully been used since. Their Compact Strip Production (CSP) was the first commercial system of integrated casting and rolling. The first such industrial installation was located at Nucor's in Crawfordsville. Nowadays, there are many variations of that technology: ISP (Inline Strip Production), DSC (Direct Strip Casting), UTHS (Ultra-Thin Hot-Strip), ESP (Endless Strip Production) and many others. In the strip casting process, steel is cast in to a thin gage, reheated and rolled into final production a limited number of passes. Its main profit is a significant cost reduction. This is due to elimination of reheating and to the very high temperature of rolling, which significantly decreases the level of yield stress. The new technologies are characterized by drastic reduction of the manufacturing costs (low level of energy and water consumption, as well as CO<sub>2</sub> emission), high productivity and capacity, and low investment costs.

## 2. MATHEMATICAL MODEL

A comprehensive description of phenomena accompanying the simulation of slab rolling involves a system of multiple differential equations. The conditions in which liquid steels subjected to solidification and the way of strip casting have a great effect on the structure and physical steel properties. A fully three-dimensional model must be considered in order to provide broad description of material behaviour during deformation process that is run under the specified conditions. Application of 3D model is necessary, due to the fact that material subjected to rolling in extra high temperature exists in two different states of aggregation: solid and semi-solid. The areas of the mentioned phases may have complex geometrical shapes. Hence, the process requires 3D mathematical modelling as opposed to traditional plate hot-rolling where two-dimensional model of deformation suffices. The mathematical model of slab casting has to take into consideration the behaviour of both solid and semi-solid materials. For this purpose, suitable equations describing plastic flow of material have to be used. Physical models of steel properties in a temperature range close to the solidus line must consider coexistence of liquid and solid phases. Development of such models is not trivial but necessary for proper interpretation of mechanical test. Furthermore, the available scientific literature lacks information about mechanical properties of steels in semi-solid state. Knowledge about the physical background of the process can be extracted from appropriately formulated mathematical models based on variational formulation and finite element discretization. The sequential model developed by the authors was then implemented in object oriented technique using C++ programming language. The considered physical continuum is inhomogeneous, due to existence of mushy regions. Thus, sufficiently precise computation is required to achieve acceptable results. Very accurate thermal, mechanical and density models are required for reliable simulation of both integrated casting and rolling and soft reduction processes. As a result, it is necessary to solve a high-dimensional system of equations. Taking into consideration the limitation of the resources of a personal computer, an accurate computation is highly exposed to long computation time.

### 2.1 Thermal model

The material behaviour above the solidus line is strongly temperature dependent. There are a few characteristic temperature levels between solidus and liquidus which decide about the steel crack resistance. The nil strength temperature (NST) is the temperature in which material strength drops to zero while the steel is being heated above the solidus temperature. Another temperature associated with NST is the strength recovery temperature (SRT), which is specified during cooling. At this temperature the material regains strength greater than 0.5 N/mm<sup>2</sup>. The nil ductility temperature (NDT) represents the temperature at which the heated material loses its ductility. The ductility recovery temperature (DRT) is the temperature at which the ductility of the material (characterized by reduction of area) reaches 5 % while it is being cooled. Above this temperature the plastic deformation, which is specific for traditional processes like rolling, is not allowed at any stress tensor configuration. The temperature has great influence on almost all material properties. Hence, a proper thermal model is extremely important. In the presented model, it was based on the general diffusion equation for a three-dimensional thermal problem, which is called Fourier-Kirchhoff equation, written in a form:

$$\frac{\partial}{\partial x} \left( \lambda_{xx} \frac{\partial T}{\partial x} \right) + \frac{\partial}{\partial y} \left( \lambda_{yy} \frac{\partial T}{\partial y} \right) + \frac{\partial}{\partial z} \left( \lambda_{zz} \frac{\partial T}{\partial z} \right) + \left( Q - \rho c_p \frac{\partial T}{\partial t} \right) = 0 \quad (1)$$

In (1)  $T$  is the temperature distribution,  $\lambda$  is the heat conduction coefficient,  $Q$  is the rate of heat generation due to plastic deformation,  $c_p$  denotes the specific heat and  $\rho$  is the density.

The applied solution was used Galerkin integration scheme, due to the fact that it gives good results for the boundary conditions existing in the rolling. But in addition to the methods used there are also other methods of integration, eg. Euler scheme and Crank-Nicholson. These methods differ from each other, constant coefficients. The solution of equation (1) has to satisfy boundary conditions. The figure presents  $\frac{1}{4}$ <sup>th</sup> of the slab

volume, which is sufficient controlled volume due to existing symmetry [5]. For the rolling process in order to track changes in temperature, mixed boundary conditions applied, consisting of a second and third boundary condition. In addition, on the end of the rolled band, was used a first boundary condition. On this surface was set at a constant temperature. The mentioned three areas are: behind the rolls (Area A), zone under the rolls (Area B) and zone in front of the rolls (Area C). Correct specification of boundary condition influences the accuracy of the solution. More information concerning the presented areas and the different boundary conditions can be found in [5]. The mathematical model describes the area is due to the fact that they exist indifferent boundary conditions. Markings shown in **Figs. 1** and **2** consecutive numbers describe the elements making up the network elements for FEM. They were placed in order to characterize the free surfaces of the individual elements, which are applied to the boundary conditions. In Area A (**Fig. 1**) can be distinguished action type III boundary conditions  $t$  and  $f$  marked contrast to the walls described the symbol  $l$  is applied boundary condition of the first kind. This area can be divided into parts, where the boundary conditions are applied on one (item 4A), two (items 2A and 3A) and three (item 1A) walls.

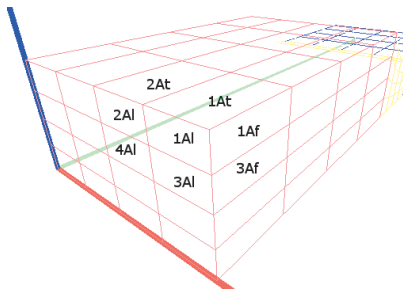


**Fig. 1** Boundary condition in Area A

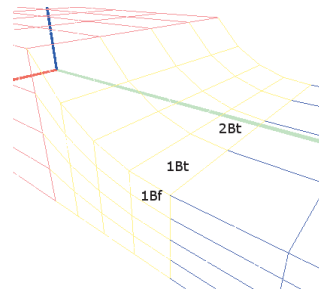


**Fig. 2** Boundary condition in Area B

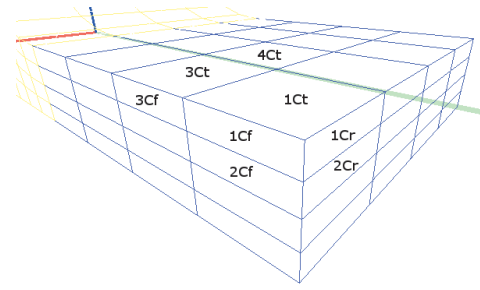


**Fig. 3** Boundary condition in Area C

Area B (**Fig. 2**) is characterized by the boundary conditions of the second kind - on the contact surface of the roll band - and the third kind - at the level of the free. The FEM mesh elements occurring in the area of the boundary conditions are applied to one (2Bt) or two sides (1Bt and 1Bt). The entire Area C (**Fig. 3**) on the surface of the free boundary condition applied is the third kind. Just as in the domain A there are grid elements in which the boundary conditions are applied to one (element 4Ct), two (elements 2C and 3C) or three (element 1C) walls.

Temperature distribution is very important. It is particularly important in the case of rolling steel slabs, which consists of solid and liquid phases as it affects other parameters. In the discussed temperature range, even small temperature changes may result in significant changes in plastic and mechanical properties. In order to show the possibilities of analysis offered by the developed simulation system, an example temperature distribution throughout the deformation zone is presented in **Fig. 4**.

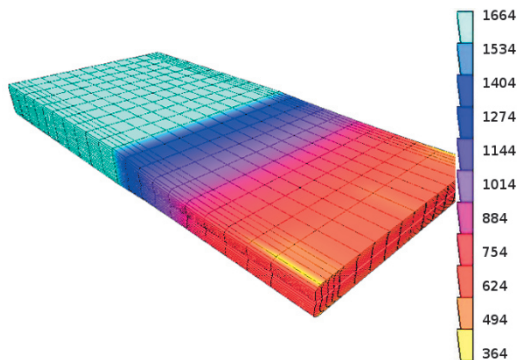


**Fig. 4** Distribution of temperature

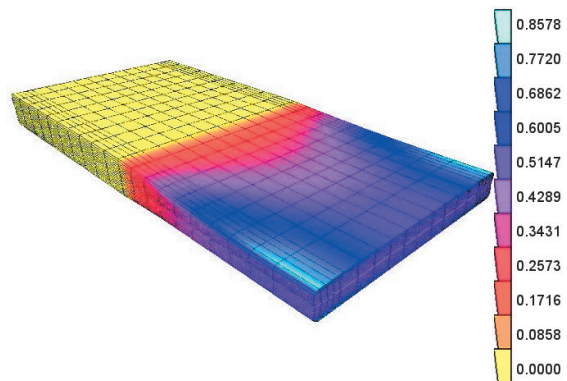


**Fig. 5** Distribution of effective strain

## 2.2 Mechanical model

The mechanical model is responsible for calculation of strain, strain rate and stress tensors as well as their distribution in the controlled volume. The deformation process has been divided into deformation steps. Mechanical solution is based on the optimization of appropriate work functional that depends on a number of parameters. The rigid-plastic formulation has been used to fulfil the Levy-Mises flow law. The work functional subjected to optimization in subsequent steps of deformation, consists of three main parts and can be written as follows:

$$W = \underbrace{\int_V \sigma_i \Delta \varepsilon_i dV}_{W_\sigma} + \underbrace{\int_V \lambda \left( \Delta \varepsilon_x + \Delta \varepsilon_y + \Delta \varepsilon_z - \frac{\Delta \rho}{\rho} \right) dV}_{W_\lambda} + \underbrace{\frac{m}{\sqrt{3}} \int_S \sigma_y \bar{\Delta} dS}_{W_f} \quad (6)$$

In equation (6)  $W_\sigma$  is the plastic work,  $W_\lambda$  is the penalty for failure to meet either the incompressibility or mass conservation condition. Both of them are responsible for the volume changes of the deformation zone. Finally,  $W_f$  is the work of friction forces. In the relation (6)  $\sigma_i$  is the effective stress which is calculated using unique yield stress functions developed by the authors [6, 7, 8]. The variable  $\lambda$  is the coefficient matching the hydrostatic stress,  $\Delta \varepsilon_i$  the effective strain increment,  $\Delta \varepsilon_x$ ,  $\Delta \varepsilon_y$ , and  $\Delta \varepsilon_z$  are the step increments of strain tensor components,  $\Delta \rho$  describes the density changes,  $\bar{\Delta}$  is the relative local displacement of metal and tool whilst  $m$  denotes the friction factor. In case of material incompressibility the work  $W_\lambda$  disappears step by step while the optimization is in progress. The sum of the three presented work components given by relationship (6) is the basis of the solution for both solid and mushy material. The discretization of the mechanical problem and the solution has been performed in usual finite-element manner [5]. **Fig. 5** shows example deformation of mesh of elements. It also presents distribution of effective strain. Lower values of this quantity are observed in the roll entry area in section, which has been minimally deformed. In the roll gap, the value of the parameter increases to a level of 0.42. The greatest values of effective strain are located just beneath the surface of the slab in its central part.

## 2.3 Variable density model

Density is one of the critical factors affecting both the temperature and the mechanical model and has to be taken into consideration. Its changes that occur with the progressive variations in physical state of steel are ruled by three main phenomena: the formation of the solid phase as a result of solidification, thermal shrinkage of solid and liquid phases and the movement displacement of the liquid phase in the matrix forming a porous solid phase. The derivative of the density with respect to time during solidification is dependent on the fraction of solid phase and can be calculated according to equation no (7):

$$\frac{\partial \rho}{\partial t} = (\rho_s d_s + \rho_l d_l) \left( \frac{\rho_s}{\rho_l} - 1 \right) \frac{\partial d_s}{\partial t} \quad (7)$$

where:  $\rho_s$  - density of the solid phase,  $\rho_l$  - density in the liquid phase,  $d_l$  - volume fraction liquid phase.

Changes of density due to thermal contraction can be described by the following relationship (8):

$$\frac{\partial \rho}{\partial t} = (\beta_s \rho_s d_s + \beta_l \rho_l d_l) \frac{\partial T}{\partial t} \quad (8)$$

where:  $\beta_s$  - volume contraction in the solid phase,  $\beta_l$  - volume contraction in the liquid phase.

Influence of variable density complicates the solution. In this paper, it is assumed that the solidification zone is composed of a porous material with laminar flow of molten metal. The area where material is porous, is characterized by the following temperature range:  $\Delta T_{ZS} = T_{lik}^* - T_{sol}^*$ , wherein  $T_{lik}^* < T_{lik}$  and  $T_{sol}^* > T_{sol}$

where:  $\Delta T_{ZS}$  - replacement temperature,  $T_{lik}^*$  - replacement temperature of liquidus,  $T_{sol}^*$  - replacement temperature of solidus,  $T_{lik}$  - liquidus temperature,  $T_{sol}$  - solidus temperature.

Density changes caused by liquid phase flow through a porous medium consisting of solid phase skeleton can be expressed taking into account the Darcy flow law (9):

$$\frac{\partial \rho}{\partial t} = -\rho_l d_l \nabla v \quad (9)$$

where velocity  $v$  is given by (10):

$$v = -\xi_{op} \nabla (p - \rho_l g h) \quad (10)$$

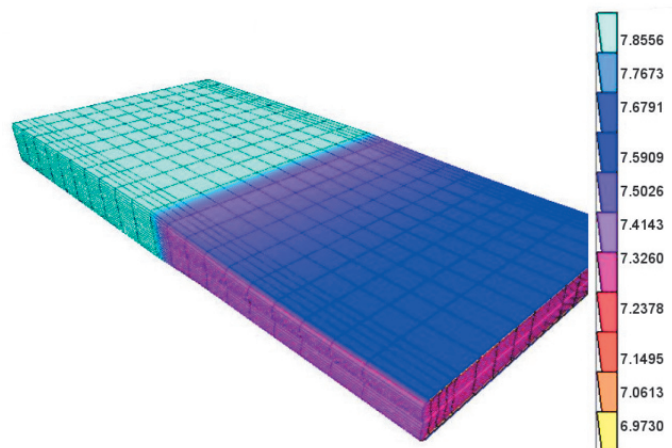
Symbols used in equation (10) denote:  $\xi_{op}$  the coefficient of permeability of a porous medium and  $h$  the distance between solid particles. The relative velocity and pressure in both the equations (9) and (10) introduce large computational problems. The total derivative of density in any small area of the body with respect to time is a sum of equations (7), (8) and (9).

$$\frac{\partial \rho}{\partial t} = (\rho_s d_s + \rho_l d_l) \left( \frac{\rho_s}{\rho_l} - 1 \right) \frac{\partial d_s}{\partial t} - (\beta_s \rho_s d_s + \beta_l \rho_l d_l) \frac{\partial T}{\partial t} - \rho_l d_l \nabla v \quad (11)$$

The average porosity in a slab node can be calculated according to the expression  $P_{SR} = \frac{\rho_s - \rho_l}{\rho_s} \cdot 100\%$ .

The theoretical model of density changes is complex and requires numerical solution of Darcy and Navier-Stokes equations, which demand processing time and memory. **Fig. 6** presents a graph of density distribution on the slab surface. As can be seen, the greatest density of the metal occurs in the area located at back end of the roll gap. In the roll gap, density is lower and rises at the exit from the roll gap. Considering the density changes along the slab height, one can see that value of this parameter is proportional to the distance to the plate center.

**Fig. 6** The density distribution of the metal in the deformed strand



## CONCLUSIONS

The paper discusses the problem of computer simulation of deformation of semi-solid steels. Three basic mathematical models are presented that subject to appropriate boundary conditions lead to computation of temperature field, strain and stress tensors and density distribution in slabs in the presence of solid and semi-solid phases. Computer simulation and pertinent experimental work lead to the following conclusions:

- Modeling the temperature field and deformation of steel in the temperature range which is close to solidus is very difficult. It requires overcoming a number of problems related to very high temperature of the rolling process and material properties specific to the considered temperature range.
- The mushy steel behaviour is very temperature sensitive. Even small changes in temperature result in significant variation of thermo-physical parameters that have critical influence on the computation results.
- In some cases, the solution fails to converge which leads to incorrect result of the simulation.

An additional remark affects the huge linear system required by the solution. It requires super computers or clusters consisting of large number of computational nodes with high-speed interconnect. The latter solution is commonly used due to financial efficiency as well as the cluster network capacity.

## ACKNOWLEDGEMENTS

***The project has been supported by the Polish National Science Centre, Decision number: DEC-2011/03/D/ST8/04041.***

## REFERENCES

- [1] KOPP R., CHOI J., NEUDENBERGER D. *Simple compression test and simulation of an Sn-15% Pb alloy in the semi-solid state*, J. Mater. Proc. Technol., vol. 135, 2003, pp. 317-323.
- [2] MODIGELL M., PAPE L., HUFSCHMIDT M. *The rheological behaviour of metallic suspensions*, Steel Research Int., vol. 75, 2004, pp. 506-512.
- [3] JING Y.L., SUMIO S., JUN Y. *Microstructural evolution and flow stress of semi-solid type 304 stainless steel*, J. Mater. Proc. Technol., vol. 161, 2005, pp. 396-406.
- [4] JIN S. D., HWAN O.K. *Phase-field modelling of the thermo-mechanical properties of carbon steels*, Acta Materialia, vol. 50, 2002, pp. 2259-2268.
- [5] JĘDRZEJCZYK D. *Przestrzenny termomechaniczny model walcowania w stanie półciekłym*, PhD thesis, AGH-University, Kraków (2008), (in Polish).
- [6] HOJNY M., GLOWACKI M. *Computer modelling of deformation of steel samples with mushy zone*, Steel Research Int., vol. 79, 2008, pp. 868-874.
- [7] GLOWACKI M., HOJNYM. *Inverse analysis applied for determination of strain-stress curves for steel deformed in semi-solid state*, Inverse Problems in Science and Engineering, vol.17, 2009, pp. 159-174.
- [8] HOJNY M., GLOWACKI M. *The methodology of strain - stress curves determination for steel in semi-solid state*, Archives of Metallurgy and Materials, vol. 54, 2009, pp.475-483.